Measuring Implosion Dynamics through ρR Evolution in Inertial-Confinement Fusion Experiments

R. D. Petrasso,* J. A. Frenje, C. K. Li, F. H. Séguin, J. R. Rygg, B. E. Schwartz, and S. Kurebayashi
Plasma Science and Fusion Center, Massachusetts Institute of Technology, Cambridge, Massachusetts 02139

P. B. Radha, C. Stoeckl, J. M. Soures, J. Delettrez, V. Yu. Glebov, D. D. Meyerhofer,† and T. C. Sangster
Laboratory for Laser Energetics, University of Rochester, Rochester, New York 14623
(Received 6 September 2002; published 6 March 2003)

The areal density (ρR) of D^3He filled plastic capsules imploded at OMEGA has been measured at shock coalescence (1.7 ns) and, 400 ps later, during compressive burn, through the energy downshift of 14.7-MeV D^3He protons. In this time interval, the azimuthally averaged ρR changes from 13 ± 2.5 to 70 ± 8 mg/cm^2. The experiments demonstrate that fuel-shell mix is absent in the central regions at shock coalescence, and that the shell has no holes during compressive burn. We conjecture that ρR asymmetries measured during compressive burn may be seeded by the time of shock coalescence.

DOI: 10.1103/PhysRevLett.90.095002 PACS numbers: 52.57.–z, 52.25.Tx, 52.50.Jm, 52.70.Nc

Proper assembly of capsule mass in inertial confinement fusion (ICF) implosions is of fundamental importance for achieving ignition [1–3], and experimental information about implosion dynamics is crucial both for understanding how assembly occurs and for critically evaluating numerical simulations. Without carefully tailored assembly of the fuel, hot-spot ignition planned for the National Ignition Facility (NIF) [1–4] and the Laser Megajoule Facility (LMJ) [5] will fail. Hot-spot ignition relies on shock coalescence to "ignite" the hot spot, followed by propagation and burn of the compressed "shell" material (compressive burn). The relationship between these events must be understood to ensure the success of ICF ignition. To elucidate these issues, we report on gated measurements of areal density (ρR) at pivotal moments during implosions: first at shock coalescence, and then 400 ps later during compressive burn. These measurements were accomplished through the use of 14.7-MeV protons generated by the fusion of the fuel constituents deuterium (D) and helium (^{3}He), in imploding capsules with 24-μm-thick plastic (CH) shells [6,7]. An accurate determination of ρR evolution and asymmetry is made by measuring the proton energy downshift at different times and in many different directions.

Earlier measurements of ρR utilizing primary 14.7-MeV protons [6–8] and secondary protons [9] concentrated on properties and dynamics during compressive burn for implosions of capsules with 20-μm-thick CH shells. These studies included ρR asymmetries [8–10], fuel-shell mix [11–14], and the effects of beam smoothing upon fuel ρR [8,11,15]. In addition, x-ray absorption techniques [16] have been used to study aspects of ρR modulations at peak compression and during decompression.

Direct-drive implosions were conducted on OMEGA, with 60 beams of frequency-tripled (351 nm) UV light in a 1-ns square pulse and total energy of 21.6 kJ [17]. Full smoothing of the laser beams was used [11], and beam-to-beam energy imbalance was typically $\leq 5\%$ rms. Two types of hydrodynamically similar capsules were used, all with nominal diameters of 940 μm and shell thicknesses of 24 μm. CH-shelled capsules were filled with approximately 6 atm of D_2 and 12 atm of ^{3}He. Capsules with shells of CD (or 1 μm of CD inside of 23 μm of CH) were filled with approximately 20 atm of ^{3}He. The principal diagnostics for this work were high-resolution, charged-particle spectrometers simultaneously viewing each implosion from different directions (the spectrometers and their properties are described in Ref. [7]). In addition, the neutron temporal diagnostic measured the D fusion burn histories [18] on hydroequivalent D_2 implosions.

The following reactions occur in imploding capsules fueled with D and ^{3}He:

$$D + D \rightarrow p(3.0\ \text{MeV}) + T(1.0\ \text{MeV}), \quad (1)$$

$$D + D \rightarrow n(2.5\ \text{MeV}) + {}^3\text{He}(0.8\ \text{MeV}), \quad (2)$$

$$D + {}^3\text{He} \rightarrow p(14.7\ \text{MeV}) + \alpha(3.6\ \text{MeV}). \quad (3)$$

This analysis uses the high-energy proton of Reaction (3) because it can easily penetrate the larger ρR during compressive burn while, in contrast, the 3.0-MeV protons of Reaction (1) are ranged out. Figure 1 shows proton spectra obtained simultaneously at five different viewing angles for shot 24811. In each spectrum, two distinct peaks are clearly evident. The narrow, higher-energy peak is associated with the burn of duration $\sim$40 ps at shock coalescence, while the broader, lower-energy peak is associated with the $\sim$150 ps compressive burn which occurs about 400 ps after the shock [19]. For each of the two peaks in each spectrum, the average energy

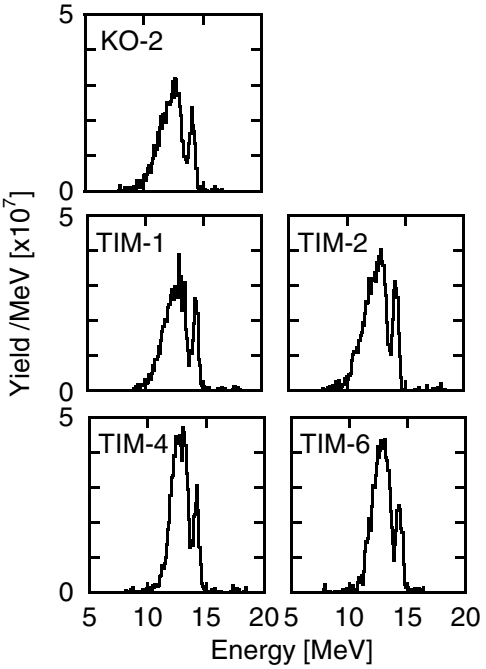

FIG. 1. Spectra of high-energy protons generated from the fusion of D and ^{3}He in an imploding ICF capsule (shot 24811). The spectrometers viewed the implosion from five different directions; each plot is identified by the OMEGA port used (Ref. [7] shows a port diagram). The narrow high-energy peak is associated with shock-coalescence burn, the broad low-energy peak with compressive burn.

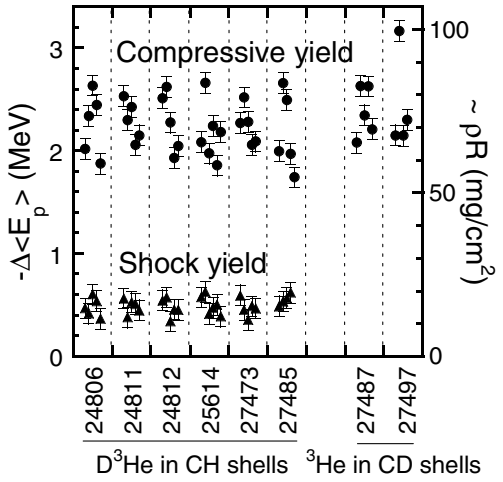

FIG. 2. The average energy downshifts (from 14.7 MeV) for the shock and compression burn peaks of each spectrum from shot 24811 (as shown in Fig. 1) and from several others. From plasma stopping power calculations [20], values of $\langle \rho R \rangle$ can be associated with the plotted values of ΔE_p, and the right-hand vertical axis scale is meant to show the approximate correspondence (Table I lists more exact values for averages over groups of shots).

downshift of the 14.7 MeV protons was evaluated and is shown in Fig. 2 along with data from several other shots. Through the use of plasma stopping power calculations [20], these energy downshifts are related to the capsule ρR (Fig. 2 and Table I). The capsule ρR at shock coalescence, which occurs 1.7 ± 0.1 ns after the beginning of the 1-ns laser pulse when no electric fields are present [21], is 13.0 ± 2.5 mg/cm^2. During compressive burn, the average ρR has increased to 70 ± 8 mg/cm^2. Since the temperature of the shell is at or below 1 keV at both shock and compression times, and since nearly all energy loss occurs through the shell [6,9], these ρR determinations are insensitive to exact values of the evolving temperature and density [20]. Table I summarizes the data of Fig. 2, which also show that asymmetries as large as 30 mg/cm^2 in areal density exist during compressive burn in these implosions. This effect has been reported for capsules with 20-μm-thick shells [8,9] and for cryogenic capsules [9].

The ion temperature at shock burn can be measured from the spectra. As shown in Fig. 3, the shock peak is well fit by a Gaussian. After accounting for the effects of the instrument response [6,7], a Doppler-derived ion temperature of 6 ± 1 keV is obtained. This temperature is higher than the neutron-derived Doppler-width temperature characterizing the compressive burn, which is about 3 keV. This method of temperature determination from the width of the 14.7-MeV proton spectrum has been previously used for thin-shell, high-temperature implosions [6]. At shock burn (for thick shell implosions), the shell is relatively "thin," the shock-induced ion temperature is relatively high, and the duration (~ 40 ps) is sufficiently short that little evolution in ρR occurs. In

TABLE I. Values of $\langle \rho R \rangle$ inferred from measured D^{3}He proton energy losses (calculated with the slowing-down formalism of Ref. [20], using energies averaged over all available spectra for each shot). For capsules with D^{3}He fuel and CH shells, it was assumed that the slowing was dominated by CH at $T_e \leq 1$ keV and $\rho = 2$ g/cm^3 at shock coalescence or 20 g/cm^3 at compression burn. For capsules with ^{3}He fuel in CD shells, which produce no shock yield, it was assumed that the slowing was dominated by CD at $T_e \leq 1$ keV and $\rho = 20$ g/cm^3. The "$\pm$" refers not to measurement uncertainties but to the standard deviation about the mean of individual measurements for each shot.

Shot	Fuel	Shell	$\langle \rho R \rangle_{\text{shock}}$ (mg/cm^2)	$\langle \rho R \rangle_{\text{comp}}$ (mg/cm^2)
24806	18 atm D^{3}He	24 μm CH	13.2 ± 2.6	70.6 ± 9.7
24811	18 atm D^{3}He	24 μm CH	13.3 ± 2.0	71.6 ± 6.1
24812	18 atm D^{3}He	24 μm CH	13.0 ± 2.5	71.1 ± 9.2
25614	18 atm D^{3}He	24 μm CH	13.7 ± 2.6	67.6 ± 6.7
27473	18 atm D^{3}He	24 μm CH	12.9 ± 2.3	70.1 ± 5.8
27485	18 atm D^{3}He	24 μm CH	15.2 ± 1.6	67.8 ± 12.1
27474	20 atm ^{3}He	24 μm CD	...	79.5 ± 8.3
27479	20 atm ^{3}He	24 μm CD	...	81.5 ± 16.4

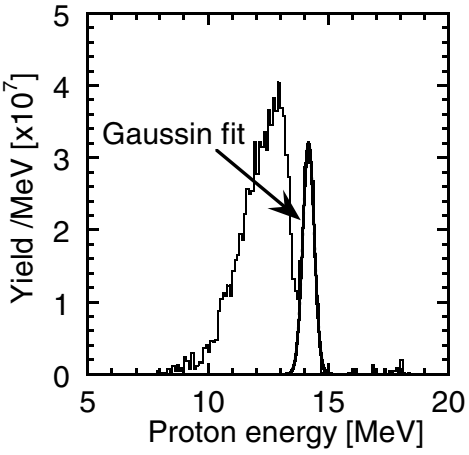

FIG. 3. A shock-induced ion temperature can be determined by fitting a Gaussian to the shock peak, correcting for the instrument response, and assuming Doppler broadening. For this spectrum the result is 6.8 keV, and the mean for all spectra from this shot (24811) is 6 keV with a standard deviation of 1 keV.

contrast, the compression burn peak for the protons (as noted previously [6]) is far wider than the Doppler width and, the effects of measured asymmetry [6–8] and geometry [7] not withstanding, largely reflects ρR evolution over the compressive burn ($\sim$ 150 ps).

To validate our interpretation that the high-energy peak (Fig. 1) is due to shock coalescence, and to explore other important aspects of implosion physics, a second series of implosions was performed using a hydrodynamically similar capsule with 20 atm of ^{3}He in a 24-μm-thick CD shell. Spectra from these implosions [see the example in Fig. 4(b)] show a single compression peak downshifted in energy by about the same amount as measured in the first series of experiments [see Fig. 4(a)]. Notably absent, however, is the shock peak in Fig. 4(a) that occurs between 14 and 15 MeV. This means that no D from the shell has mixed into the central, high-temperature region at shock time [22]. Conversely, by the time of compressive burn mixing of the CD shell with the ^{3}He must have occurred (Fig. 4) in order for D^{3}He reactions to be present (see Refs. [11–14] for more discussion of mix).

The spectrum of Fig. 4(b) can also be directly interpreted to mean that, at least for these implosions, the shell is not riddled with holes during compressive burn even though low-mode asymmetries exist (Fig. 2). If there were holes there would be a high-energy peak in Fig. 4(b). This issue is important since concern exists as to whether shell breakup, as a consequence of Rayleigh-Taylor instability, occurs prior to burn propagation and ignition, thereby quenching ignition.

To improve our understanding of the physical processes and to test the validity of 1D hydrodynamic simulations in realistic circumstances, we show a comparison of

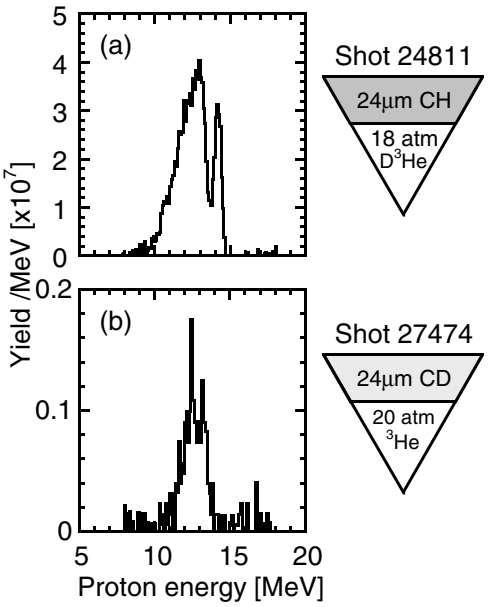

FIG. 4. The shock-induced burn which is present in plot (a) is absent when the fuel is changed to pure ^{3}He within a CD shell [plot (b)], although the compressive burn is still present because of fuel-shell mix. Besides validating the identification of the shock-induced peak, these data demonstrate the absence of shell-fuel mix in the central regions of the capsule at shock coalescence.

simulated [23] and experimental charged-particle spectra in Fig. 5. The basic structure of the experimental data is reproduced reasonably well by the simulation, which used a flux limiter of 0.06 [24,25]. Of particular relevance is the comparison at shock coalescence since, as experimentally demonstrated, the effects of mix are very minimal and 1D simulations should be at their most accurate as they do not include mix effects. In this context, the ratio of experimental shock yield to theoretical is about 60%;

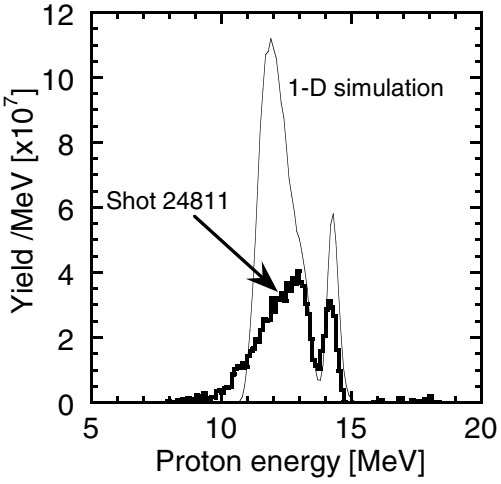

FIG. 5. A comparison of 1D simulation to data from shot 24811.

the predicted ρR is 10.5 mg/cm^2 while the experimental value is 13 ± 2.5 mg/cm^2; the predicted shock temperature is 8 keV, while the measurement is 6 ± 1 keV; and the predicted interval between shock and compression burn is 500 ps, while the measured interval is about 400 ps. If instead a larger flux limiter of 0.07 is used in the 1D simulation, as some workers have advanced [26], the ratio of experimental shock yield to the theoretical value is reduced to 30%; the predicted ρR increases slightly to 11.0 mg/cm^2; the predicted temperature increases to 10 keV; and the interval between shock and compression is reduced to about 400 ps. As shock timing and coalescence are critical to ignition at the NIF and the LMJ [1–5], experiments that test the limits of validity of simulation codes, as described herein, will be helpful to this endeavor. Additionally, it seems entirely plausible that similar measurements could be made at the NIF at various phases in the development and testing of preignition capsules, if not ignition capsules themselves.

In summary, we have presented the first measurements of ρR evolution occurring in ICF implosions. In the 400 ps interval between shock coalescence and compression burn, the azimuthally averaged ρR changed from 13.0 ± 2.5 to 70 ± 8 mg/cm^2. The experiments demonstrated that fuel-shell mix has not occurred in the central regions of the imploding capsule at shock coalescence, and that the shock-induced temperature is about 6 keV. As mix is inconsequential at this stage of the implosion, these and other measured parameters offer a sensitive test of 1D shock physics simulations. The experiments further demonstrated that, at least for these types of implosions, gaps and holes do not riddle the shell at compression burn.

Several intriguing avenues exist for advancing these measurements and our understanding of implosion dynamics. As ρR is sufficiently small at shock coalescence, 3.0-MeV protons from Reaction (1) will readily penetrate the shell and lead, in principle, to a second independent measurement of the shell ρR at that instant. Such experiments, as well as higher-accuracy spectrometers for D^3He fusion reactions, are being planned. With more accurate ρR measurements at shock coalescence, studies will be undertaken to establish whether ρR asymmetries exist at that time, and whether these asymmetries persist and amplify through the compression burn phase [9,10], thereby accounting for the notable asymmetries that have been measured at compression burn. In addition, because of the strength of the shock flash, highly accurate measurements of the D^3He reaction burn history are presently being implemented [27]. In combination with the spectrally resolved measurements, these new developments will make possible precise measurements of shock and compression times.

The authors express their gratitude to the OMEGA engineers and operations crew who supported these experiments, and to Dr. Peter Amendt, Dr. Nelson Hoffman, Dr. Richard Olsen, and Dr. Mordecai Rosen for very helpful comments. We thank Professor Miklos Porkolab and Professor Robert McCrory who have fostered and supported this program. This work has been supported in part by LLE (Subcontract No. P0410025G) and LLNL (Subcontract No. B313975), and by the U.S. Department of Energy Office of Inertial Confinement Fusion (Grant No. DE-FG03-99DP00300) and under Cooperative Agreement No. DE-FC03-92SF19460, the University of Rochester, and New York State Energy Research and Development Authority.

*Also Visiting Senior Scientist at LLE.
†Also Department of Mechanical Engineering, Physics and Astronomy.

[1] S. W. Haan *et al.*, Phys. Plasmas **2**, 2480 (1995).
[2] J. D. Lindl, R. L. McCrory, and E. M. Campbell, Phys. Today **45**, 32 (1992).
[3] *Energy & Technology Review* (Lawrence Livermore National Laboratory, Livermore, CA, 1994).
[4] M. D. Rosen, Phys. Plasmas **3**, 183 (1996).
[5] M. Andre, M. Novaro, and D. Schirmann, Rev. Sci. Tech. Direction Appl. Militaires **13**, 73 (1995); J. Maddox, Nature (London) **372**, 127 (1994).
[6] C. K. Li *et al.*, Phys. Plasmas **7**, 2578 (2000).
[7] F. H. Séguin *et al.*, Rev. Sci. Instrum. 74, 975 (2003).
[8] F. H. Séguin *et al.*, Phys. Plasmas **9**, 2527 (2002).
[9] F. H. Séguin *et al.*, Phys. Plasmas **9**, 3558 (2002).
[10] R. D. Petrasso *et al.*, Phys. Rev. Lett. **77**, 2718 (1996).
[11] D. D. Meyerhofer *et al.*, Phys. Plasmas **8**, 2251 (2001).
[12] D. D. Meyerhofer *et al.*, Plasma Phys. Controlled Fusion A **43**, 277 (2001).
[13] P. B. Radha *et al.*, Phys. Plasmas **9**, 2208 (2002).
[14] C. K. Li *et al.*, Phys. Rev. Lett. 89, 165002 (2002).
[15] C. K. Li *et al.*, Phys. Plasmas **8**, 4902 (2001).
[16] V. A. Smalyuk *et al.*, Phys. Rev. Lett. **87**, 155002 (2001).
[17] T. R. Boehly *et al.*, Opt. Commun. **133**, 495 (1997).
[18] R. A. Lerche *et al.*, Rev. Sci. Instrum. **66**, 933 (1995).
[19] R. D. Petrasso *et al.*, Bull. Am. Phys. Soc. **46**, 105 (2001).
[20] C. K. Li and R. D. Petrasso, Phys. Rev. Lett. **70**, 3059 (1993).
[21] It has been demonstrated that the effect of electric fields is negligible for these types of capsules driven by 1-ns-square laser pulses since shock coalescence and bang time occur hundreds of picoseconds after the laser pulse, at which time the electric field has largely decayed away.
[22] From other D^3He implosion experiments, for which the signals are similar in amplitude to those of Fig. 4(b), the presence of the shock yield is clearly visible. So the absence of the shock yield in Fig. 4(b) is not due to lack of instrument sensitivity.
[23] E. B. Goldman, LLE Report No. 16, University of Rochester, 1973.
[24] J. Delettrez, Can. J. Phys. **64**, 932 (1986).
[25] R. C. Malone, R. L. McCrory, and R. L. Morse, Phys. Rev. Lett. **34**, 721 (1975).
[26] J. Delettrez *et al.*, Bull. Am. Phys. Soc. **47**, 142 (2002).
[27] J. Frenje *et al.* (private communication).